ChemComm

Accepted Manuscript

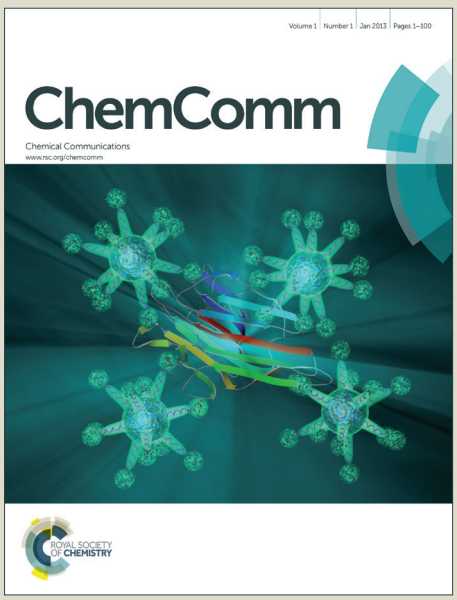

ROYAL SOCIETY OF CHEMISTRY

www.rsc.org/chemcomm

ChemComm

COMMUNICATION

Metal ion clip: fine tuning aromatic stacking interactions in multistep formation of carbazole-bridged zinc(II) complexes

Yuki Imai,[a] Tsuyoshi Kawai*[a] and Junpei Yuasa*[a,b]

Received 00th January 20xx,
Accepted 00th January 20xx

DOI: 10.1039/x0xx00000x

www.rsc.org/

A carbazole-based triple bridging ligand (LH) consisting of two imidazole moieties at 3,6 positions with a diketone unit at the carbazole nitrogen forms carbazole-bridged zinc(II) complexes with structures of $[(L^-)_4(Zn^{2+})_n]$ (n = 2–6), where the strength of aromatic stacking interactions between the carbazole rings increases with an increase in the number of Zn^{2+} ions bridged by the imidazole moieties.

The strength of aromatic stacking interactions is an important determinant in the chemical and physical properties of aromatic compounds as well as chemical and biological recognition.[1] Stacking interactions for typical aromatic-aromatic contacts are weak,[2] and normally afford only stacked (*on*) and unstacked (*off*) states in solutions. The strength of attractive interactions between aromatic units can be improved if additional interactions are involved[3] such as metal-ligand interactions.[4–7] Hence, self-assembly via metal–ligand complexation could be a unique approach to modulate stacking interactions. Previously metal–ligand directed assembly approaches containing distinct binding sites have mainly focused on the cooperative binding of metal ions for development of a nonlinear response to achieve "*on*/*off*" switching under specific threshold conditions,[4] or for development of excimer based turn-on fluorescence sensors.[5] Alternatively, we have recently reported metal-assisted π-association (*on*) and dissociation (*off*) of aromatic rings consisting of imidazole moieties, in which, multistep complex formation regulated by the metal ion concentration can produce only the two distinct complexes with (*on*) and without (*off*) stacked aromatic units.[8]

We report herein the fine-tuning of aromatic stacking interactions regulated by the metal ion concentration, enabling "loose" and "tight" dimer contacts between the aromatic rings for the first time. In this method hereon referred to as *metal ion clip*, three distinct potential binding sites for metal ions were introduced into a carbazole ring (LH),[9] two imidazole moieties at 3,6 positions and a diketone unit at the carbazole nitrogen, the latter of which is the stronger binding site. Diketone ligands often give L_2M type complexes through deprotonation of the α-proton when they interact with divalent cations such as zinc (II) (Zn^{2+}).[10] In such preorganization $[(L^-)_2(Zn^{2+})_m]$, the two aromatic surfaces are adjacent to each other, resulting in four distinct potential binding sites for metal ions (Scheme 1). In this paper, we demonstrate how this approach can modulate aromatic stacking interactions, enabling "loose" and "tight" dimer contacts.

Complex formation of LH with $Zn(OTf)_2$ (OTf = OSO_2CF_3) was examined with UV-vis titration experiments at two different initial LH concentrations: $[LH]_0$ = 2.0 × 10^{-5} M and 2.0 × 10^{-4} M in methanol. In the case of low initial concentration of $[LH]_0$ = 2.0 × 10^{-5} M (Fig. 1a), LH shows a biphasic UV-vis spectral change in response to the molar ratio of $[Zn^{2+}]/[LH]_0$ = 0–0.5 (red lines) and 0.5–3.1 (blue lines). The absorption band at the peak wavelength (λ_{max} = 311 nm) decreases with a clear isosbestic point at λ = 355 nm at $[Zn^{2+}]/[LH]_0$ = 0–0.5 (Fig. 1a, red lines), while the peak shoulder at around λ = 340 nm gradually increases with the increased ratio of $[Zn^{2+}]/[LH]_0$ = 0.5–3.1 (Fig. 1a, blue lines). Such biphasic UV-vis spectral changes are ascribed to stepwise complex formation[8] between LH and Zn^{2+}, a first Zn^{2+} ion binds to the diketone unit through deprotonation of the α-proton (Scheme 1a), after which the second Zn^{2+} ion is coordinated to the imidazole nitrogen above $[Zn^{2+}]/[LH]_0$ = 0.5 (Scheme 1b). Negative control experiments were conducted with a reference compound (LH') to confirm that the imidazole moieties serve as the distinct binding sites for the second Zn^{2+} ion. The reference compound (LH') has no imidazole moiety but has the diketone unit at the carbazole nitrogen (Scheme 1). LH' shows a monotonous UV-vis spectral change during the titration of Zn^{2+} with clear isosbestic points (see ESI† S2), suggesting formation of a single complex species upon binding of Zn^{2+} to the diketone unit. The negative result obtained with LH' is clear evidence that the imidazole moieties in LH act as the distinct binding site for the second Zn^{2+} ion. Then, the binding stoichiometry of LH with Zn^{2+} was estimated from the titration plot. The titration curve shows two breaks at $[Zn^{2+}]/[LH]_0$ = 0.5 and 1.0 (inset of Fig. 1a). The binding

[a] Graduate School of Materials Science, Nara Institute of Science and Technology, 8916-5 Takayama, Ikoma, Nara 630-0192, Japan. Fax: (+81) 743-72-6179; E-mail: yuasaj@ms.naist.jp; tkawai@ms.naist.jp
[b] PRESTO, Japan Science and Technology Agency, Kawaguchi, 332-0012, Japan

† Electronic Supplementary Information (ESI) available: [Experimental section, titration of LH' with Zn^{2+}, excitation spectra, NMR titration of LH with Zn^{2+}, titration of LH with triflic acid, calculated isotopic distributions, temperature dependence of emission spectra, and monomer-dimer simulation]. See DOI: 10.1039/x0xx00000x

stoichiometry of $[Zn^{2+}]/[LH]_0 = 0.5$ and 1.0 should correspond to $(L^-)_2(Zn^{2+})$ and $(L^-)_2(Zn^{2+})_2$, respectively.

In the case of high initial concentration of $[LH]_0 = 2.0 \times 10^{-4}$ M, LH shows three-step spectral changes during the titration of Zn^{2+} (Fig. 1b), where the titration curve also reveals two breaks at around $[Zn^{2+}]/[LH]_0 = 0.5$ and 1.0 (Fig. 1b inset). Upon addition of more than 1.3 equivalent of Zn^{2+} (Fig. 1b green lines), the absorption band at the peak wavelength (λ_{max} = 311 nm) gradually decreases with the increased ratio of $[Zn^{2+}]/[LH]_0$ along with the development of an absorption tail observed at wavelengths longer than 360 nm. This spectral patterning resembles that arising from exciton coupling between adjacent carbazole chromophores in a face-to-face position.[12]

Multistep complex formation of LH with Zn^{2+} was also investigated by fluorescence titration under the two different conditions ($[LH]_0 = 2.0 \times 10^{-5}$ and 2.0×10^{-4} M). In the case of low initial concentration ($[LH]_0 = 2.0 \times 10^{-5}$ M, Fig. 1c), the emission peak at 388 nm due to carbazole monomer fluorescence decreases monotonously with the increased ratio of $[Zn^{2+}]/[LH]_0$ (0–2.9 eq), where a two-step saturation curve is also present in the titration plot at $[Zn^{2+}]/[LH]_0 = 0.5$ and 1.0 (inset of Fig. 1c). Conversely, when the initial concentration of LH is increased 10-fold ($[LH]_0 = 2.0 \times 10^{-4}$ M), the carbazole fluorescence peak at 388 nm deceases with concomitant increase of a broad structureless emission band at

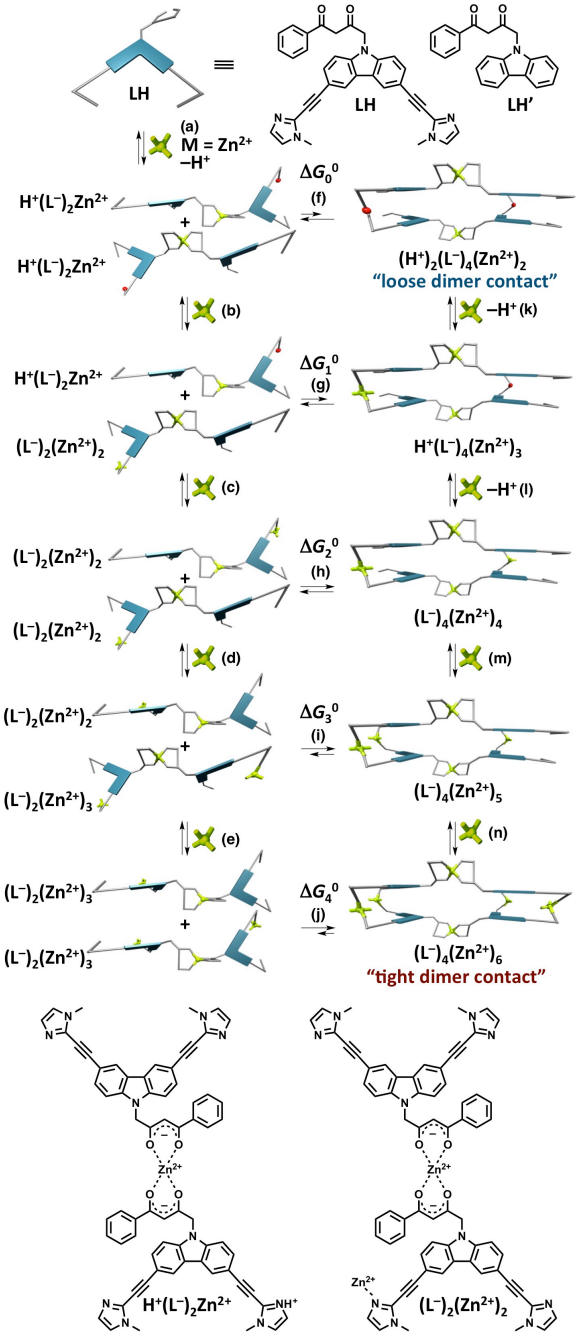

Scheme 1 (a)-(e) Multistep complex formation between LH and Zn^{2+}. (f)-(j) Stacked–unstacked equilibrium. (k)-(n) Sequential binding of Zn^{2+} to the stacked complexes. Structures of $H^+(L^-)_2Zn^{2+}$ and $(L^-)_2(Zn^{2+})_2$.

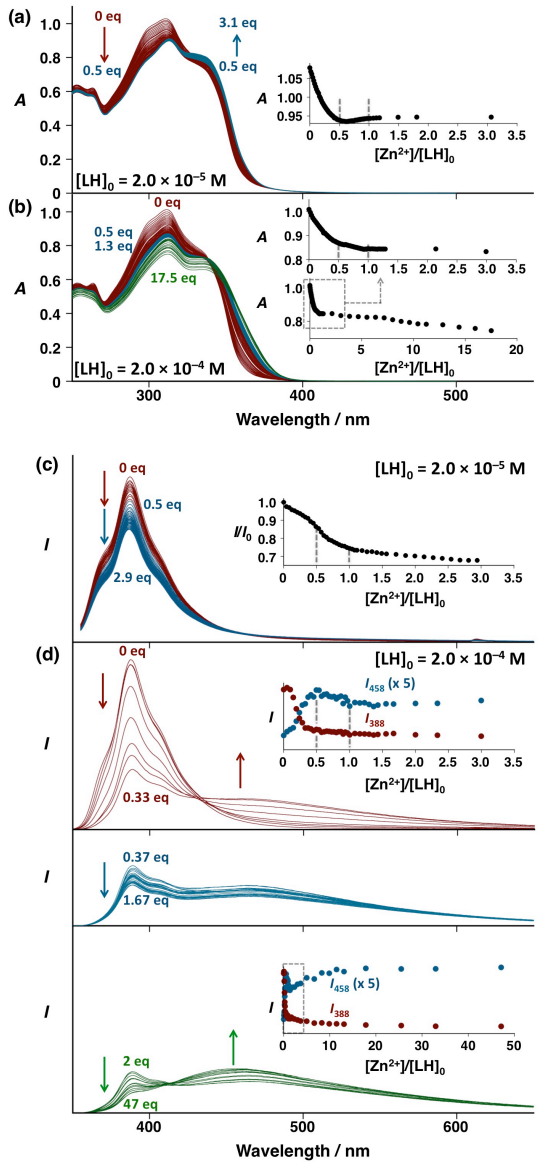

Fig. 1 UV-vis absorption spectra of LH (a) (2.0×10^{-5} M) and (b) (2.0×10^{-4} M) (1 mm path-length) in the presence of Zn^{2+} in methanol at 298 K. Emission spectra of LH (c) (2.0×10^{-5} M) and (d) (2.0×10^{-4} M) in the presence of Zn^{2+} in methanol at 298 K. Excitation wavelength: (c) λ_{ex} = 330 nm and (d) 340 nm. Insets: Plots of absorbance at (a)(b) 311 nm (c) relative emission intensity (I/I_0) at 388 nm, and (d) emission intensity at 388 nm (I_{388}: red circles) and 458 nm (I_{458}: blue circles) vs. $[Zn^{2+}]/[L]_0$.

around 458 nm in the concentration range of $[Zn^{2+}]/[LH]_0$ = 0–0.33, where a clear iso-emission point is observed at λ = 431 nm (Fig. 1d red lines).[13,14] The broad emission band at around 458 nm is characteristic of the excimer formed by face-to-face stacking of carbazole rings.[12] In the concentration range of $[Zn^{2+}]/[LH]_0$ = 0.37–1.67, the emission intensity decreases in whole wavelength region with the increased ratio of $[Zn^{2+}]/[LH]_0$ (Fig. 1d blue lines). At higher Zn^{2+} concentrations ($[Zn^{2+}]/[LH]_0$ = 2–47), the monomer carbazole fluorescence at shorter wavelength is diminished almost completely, and the carbazole excimer emission at longer wavelength is enhanced with a clear iso-emission point at λ = 413 nm (Fig. 1d green lines).[14] The titration plots are shown in the inset of Fig. 1d, where there are also two breaks at $[Zn^{2+}]/[LH]_0$ = 0.5 and 1.0. This is a clear indication of 2:1 (or 4:2) and 2:2 (or 4:4) binding stoichiometry even at the high initial concentration of LH (2.0×10^{-4} M). The remarkable difference in spectral features resulting from the difference in the initial concentration of LH (2.0×10^{-5} and 2.0×10^{-4} M) clearly suggests the existence of a stacked–unstacked equilibrium of the preorganized complexes $[(L^-)_2(Zn^{2+})_m]$ (Scheme 1f-j).[15]

Scheme 1 explains the stacked–unstacked equilibrium. Upon addition of less than 0.5 equivalent of Zn^{2+} (Scheme 1a), the first Zn^{2+} ion is coordinated to form $(L^-)_2(Zn^{2+})$ through deprotonation of LH. This process may be accompanied with partial protonation of the imidazole nitrogen atoms. The protonation constant (K) was estimated by UV-vis titration of LH with triflic acid (see ESI† S5). The determined-protonation constant $K = 9.4 \times 10^4$ M^{-1} enables us to estimate that ca. 50% of the imidazole nitrogen undergoes protonation in the methanol solution of $[LH]_0 = 2.0 \times 10^{-4}$ M containing 0.5 equivalent of Zn^{2+} (1.0×10^{-4} M). The stacked–unstacked equilibrium between $(H^+)_2(L^-)_4(Zn^{2+})_2$ and $H^+(L^-)_2(Zn^{2+})$ (Scheme 1f) gives both the monomer carbazole fluorescence and the carbazole excimer in the concentration range of $[Zn^{2+}]/[LH]_0$ = 0–0.33 (Fig. 1d red lines). The protons bound to the imidazole nitrogen should be gradually replaced by Zn^{2+} (Scheme 1k and 1l) during the concentration range of $[Zn^{2+}]/[LH]_0$ = 0.5–1.0, since the titration curve showed two breaks at $[Zn^{2+}]/[LH]_0$ = 0.5 and 1.0 (inset of Fig. 1b and 1d, vide supra). For this reason, no distinct spectral change was observed in this concentration region (Fig. 1d blue lines, vide supra). At higher Zn^{2+} concentrations, the excess Zn^{2+} ion should interact with the free imidazole nitrogen to give $(L^-)_4(Zn^{2+})_6$ (Scheme 1n), which stabilizes the stacked state and shifts the stacked–unstacked equilibrium to the stacked complex. Thus the carbazole excimer was enhanced in the concentration region of $[Zn^{2+}]/[LH]_0$ = 2–47 (Fig. 1d green lines, vide supra). The structure of $(L^-)_4(Zn^{2+})_6$ was optimized at B3LYP/LANL2DZ, where the vacant sites of Zn^{2+} were occupied by methanol molecules to satisfy tetrahedral geometry around Zn^{2+} (Fig. 2). The model structure suggests that the Zn^{2+} ions bridged by the imidazole moieties bring the two carbazole rings in a face-to-face position (Fig. 2), which is consistent with the above assumption. The ethyne spacer allows the rotational flexibility around imidazole groups. This appears to play an important role in the face-to-face arrangement of the carbazole rings.

The stacked complex, $(L^-)_4(Zn^{2+})_4$ was successfully identified by the positive-ion ESI mass of a methanol solution of LH (1.3×10^{-3} M) containing 1 equivalent of $Zn(OSO_2CF_3)_2$ (Fig. 3). The mass

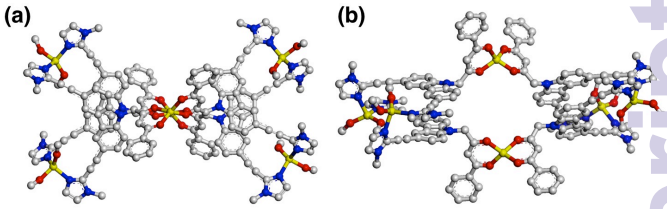

Fig. 2 The structure of $(L^-)_4(Zn^{2+})_6(CH_3OH)_8$ optimized at B3LYP/LANL2DZ: (a) top view and (b) side view.

signal at m/z = 1345.2 (red circles) corresponds to $\{[Zn_4(L)_4](OSO_2CF_3)_2\}^{2+}$, which is largely overlapped with that of $\{[Zn_2(L)_2](OSO_2CF_3)\}^+$ (1:1 ratio). Characteristic distribution of isotopomers in those signals agrees closely with their calculated isotopic distributions (inset of Fig. 3). The fragment mass signals were also found at m/z = 1707.03 (L_2M_3), 2092.27 (L_3M_3), and 2454.10 (L_3M_4). The unstacked complexes were detected at m/z = 1283.28 (L_2M_2) with a weak signal at m/z = 1495.16 (L_2M).

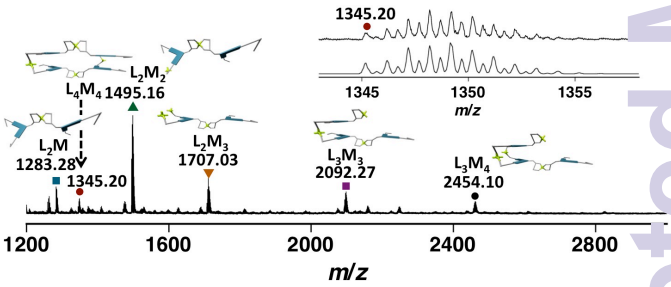

Fig. 3 Positive-ion ESI MS of a solution of LH (1.3×10^{-3} M) in methanol in the presence of $Zn(OSO_2CF_3)_2$ (1.3×10^{-3} M). Inset shows isotopically resolved signals at m/z = 1345.2 and the calculated isotopic distributions for $\{[Zn_4(L)_4](OSO_2CF_3)_2\}^{2+}$ combined with $\{[Zn_2(L)_2](OSO_2CF_3)\}^+$ (1:1 ratio). m/z = 1283.28: $\{[Zn(L)_2H_2](OSO_2CF_3)\}^+$, m/z = 1495.16: $\{[Zn_2(L)_2H](OSO_2CF_3)_2\}^+$, m/z = 1707.03: $\{[Zn_3(L)_2](OSO_2CF_3)_3\}^+$, m/z = 2092.27: $\{[Zn_3(L)_3](OSO_2CF_3)_2\}^+$, and m/z = 2454.10: $\{[Zn_4(L)_3](OSO_2CF_3)_4\}^+$ (see ESI† S6).

In light of these results, we tried to estimate the strength of aromatic stacking interactions by temperature dependence of emission spectra of LH (2.0×10^{-4} M) in the presence of 0.5, 0.9, and 50 equivalents of Zn^{2+} (Fig. 4a-c, respectively), which correspond to ΔG_0^0, ΔG_2^0, and ΔG_4^0, respectively (Scheme 1f, 1h and 1j, respectively). In the presence of 0.5 and 0.9 equivalents of Zn^{2+} (Fig. 4a and 4b, respectively), the excimer emission intensity normalized by the monomer fluorescence intensity (I_{464}/I_{390}) decreases with increasing temperature (Fig. 4d and 4e), indicating that the stacked complexes $[(L^-)_4(Zn^{2+})_n]$ are thermodynamically favored as compared to the unstacked complexes $[(L^-)_2(Zn^{2+})_n]$. In contrast, LH with 50 equivalent Zn^{2+} shows no apparent emission spectral shape change at 203–333 K, where no monomer fluorescence peak is detected over the whole temperature range (Fig. 4c). Although the strength of aromatic stacking interactions in the multistep equilibrium could be difficult to determine accurately, simple monomer-dimer simulation suggests that such insensitive temperature dependence observed at 50 equivalent Zn^{2+} (Fig. 4f) can be obtained with $-\Delta G_4^0$ larger than 10 kcal mol^{-1} (tight dimer contact, see ESI† S8). On the other hand, the temperature dependent change in the intensity ratio of the monomer fluorescence and the excimer emission observed at 0.5 and 0.9 equivalents of Zn^{2+} (Fig. 4d and

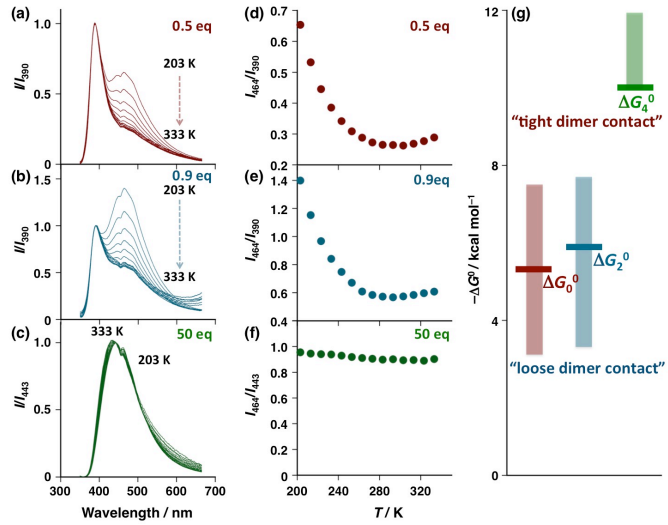

Fig. 4 Normalized emission spectra of LH (2.0×10^{-4} M) in the presence of Zn^{2+} (a) (1.0×10^{-4} M), (b) (1.8×10^{-4} M), and (c) (1.0×10^{-2} M) in methanol at 203–333 K. Excitation wavelength: λ = 340 nm. Plots of relative emission intensity (d), (e) (I_{464}/I_{390}), and (f) (I_{464}/I_{443}) *vs.* *T*. (g) Estimated ΔG_0^0, ΔG_2^0, and ΔG_4^0. The spectra are normalized at (a), (b) 390 nm and at (c) 443 nm (for non-normalized spectra, see ESI† S7).

respectively) is likely obtainable with $-\Delta G_0^0$ and $-\Delta G_2^0$ = 3–7 kcal mol^{-1} (loose dimer contact, see ESI† S8). The LH sample containing 0.9 equivalent of Zn^{2+} shows the higher intensity ratio of excimer emission at 203 K (Fig. 4a) as compared to that containing 0.5 equivalent of Zn^{2+} (Fig. 4b), indicating that $-\Delta G_2^0$ is slightly larger than $-\Delta G_0^0$. The estimated $-\Delta G^0$ values (Fig. 4g) are considerably higher than typical aromatic–aromatic interactions (ca. 2.4 kcal mol^{-1}),[2] suggesting that the metal–ligand interactions between Zn^{2+} and the imidazole moieties mainly contribute to the stability of the stacking arrangements. In contrast, the stabilization energy of the carbazole excimer should depend on the distance between the carbazole rings in the face-to-face position. In such a case, the coordination arrangements around Zn^{2+} largely contribute to the stabilization energy of the carbazole excimer.[14]

In conclusion, we have demonstrated the efficiency of the metal-ion clip method in fine-tuning aromatic stacking interactions. Sequential binding of Zn^{2+} to the imidazole moieties bridges the two preorganized complexes $[(L^-)_2(Zn^{2+})_m]$ and strengthens the stacking interaction between the carbazole rings in stages. This approach then becomes of interest in finding a way to control aromatic stacking interactions, enabling "loose" and "tight" dimer contacts between the aromatic rings.

This work was partly supported by JST-PRESTO "Molecular technology and creation of new functions"; a Grant-in-Aid for Scientific Research (C) (No. 21750147) and Scientific Research (A) (No. 21107520) from the Ministry of Education, Culture, Sports, Science and Technology, Japan.

Notes and references

1 E. A. Meyer, R. K. Castellano and F. Diederich, *Angew. Chem., Int. Ed.*, 2003, **42**, 1210 and references therein.

2 W. L. Jorgensen and D. L. Severance, *J. Am. Chem. Soc.*, 1990, **112**, 4768.

3 (*a*) H. W. Roesky and M. Andruh, *Coord. Chem. Rev.*, 200. **236**, 91; (*b*) S. L. Cockroft, C. A. Hunter, K. R. Lawson, J. Perkins and C. J. Urch, *J. Am. Chem. Soc.*, 2005, **127**, 859.

4 A. Robertson, M. Ikeda, M. Takeuchi and S. Shinkai, *Bu. Chem. Soc. Jpn.*, 2001, **74**, 883.

5 (*a*) R.-H. Yang, W.-H. Chan, A. W. M. Lee, P.-F. Xia, H.-. Zhang and K. A. Li, *J. Am. Chem. Soc.*, 2003, **125**, 2884; (*b*) M. Licchelli, L. Linati, A. O. Biroli, E. Perani, A. Poggi and D. Sacchi, *Chem.–Eur. J.*, 2002, **8**, 5161; (*c*) B. Bodenant, Fages and M.-H. Delville, *J. Am. Chem. Soc.*, 1998, **120**, 7511; (*d*) H. J. Kim, J. Hong, A. Hong, S. Ham, J. H. Lee and J. S. Kim, *Org. Lett.*, 2008, **10**, 1963; (*e*) S. Malkondu, Turhan and A. Kocak, *Tetrahedron Lett.*, 2015, **56**, 162; (*f*) M. Shellaiah, Y. H. Wu, A. Singh, M. V. Ramakrishnam Ra. and H. C. Lin, *J. Mater. Chem. A*, 2013, **1**, 1310; (*g*) L. Tang, D. Wu, X. Wen, X. Dai and K. Zhong, *Tetrahedron*, 2014, **7**. 9118.

6 (*a*) J. Yuasa and S. Fukuzumi, *J. Am. Chem. Soc.*, 2007, **129**, 12912; (*b*) J. Yuasa, T. Suenobu and S. Fukuzumi, *J. Chem. Soc.*, 2003, **125**, 12090; (*c*) J. Yuasa, T. Suenobu and S. Fukuzumi, *ChemPhysChem*, 2006, **7**, 942.

7 S. Sato, R. Takeuchi, M. Yagi-Utsumi, T. Yamaguchi, Y. Yamaguchi, K. Kato and M. Fujita, *Chem. Commun.*, 2015, **51**, 2540.

8 (*a*) T. Ogawa, J. Yuasa and T. Kawai, *Angew. Chem., Int. Ed.*, 2010, **49**, 5110; (*b*) N. Inukai, J. Yuasa and T. Kawai, *Chem. Commun.*, 2010, **46**, 3929; (*c*) N. Inukai, T. Kawai and Yuasa, *Chem.–Eur. J.*, 2014, **20**, 15159.

9 Carbazole derivatives have been extensively utilized as building blocks for metal–ligand directed self-assembly, see J.-R. Li, H.-C. Zhou, *Nature Chem.*, 2010, **2**, 893.

10 C. Nie, Q. Zhang, H. Ding, B. Huang, X. Wang, X. Zhao, S. Li, H. Zhou, J. Wu and Y. Tian, *Dalton Trans.*, 2014, **43**, 59.

11 (*a*) J. Yuasa, A. Mitsui and T. Kawai, *Chem. Commun.*, 2011, **47**, 5807; (*b*) N. Inukai, T. Kawai and J. Yuasa, *Chem. Commun.*, 2011, **47**, 9128; (*c*) N. Inukai, T. Kawai and Yuasa, *Chem.–Eur. J.*, 2013, **19**, 5938.

12 Ohkita et al extensively studied excimer formation in rigid carbazolophane, see: H. Ohkita, S. Ito, M. Yamamoto, Y. Tohda and K. Tani, *J. Phys. Chem. A*, 2002, **106**, 2140.

13 Excitation spectra recorded at 392 and 450 nm are almost identical to the absorption spectra (see ESI† S3).

14 No appreciable change in excimer emission maxima was observed during the titration (Fig. 1c and 1d), indicating no significant change in the stabilization energy of the carbazole excimer. The term "loose and tight dimer contacts" used in this study denotes the thermodynamic stability of the stacking arrangements (mainly due to the metal–ligand interactions).

15 LH (2.0×10^{-2} M) shows line broadening in NMR spectra upon addition of 0–0.2 equivalent of Zn^{2+} in CD_3OD, where the aromatic protons of the carbazole ring (C_1–H and C_4–H) show upfield shifts (see ESI† S4). The upfield shifts clearly suggest the shielding effects of the carbazole rings, a clear indication of the stacked carbazole units. In addition, the diffusion coefficient of LH ($D = 8.8 \pm 0.4 \times 10^{-10}$ m^2 s^{-1}) decreases significantly ($D = 4.3 \pm 0.8 \times 10^{-10}$ m^2 s^{-1}) in the presence of Zn^{2+}, indicating that the size of the stacked complex is larger than the unstacked complex. Precipitation was observed at the higher Zn^{2+} concentrations under these conditions due to low solubility of the stacked complexes in CD_3OD.

